Electron Charge Density Distribution from X-ray Diffraction Study of the M-Nitrophenol Compound in the Monoclinic Form

Fodil Hamzaoui [1,*], **Mokhtaria Drissi** [1], **Abdelkader Chouaih** [1], **Philippe Lagant** [2] and **Gérard Vergoten** [2]

1 Laboratoire SEA2M, Département de Chimie, Université de Mostaganem, 27000 Mostaganem, Algeria.

2 UMR CNRS 8576 Glycobiologie Structurale et Fonctionnelle, Université des Sciences et Technologies, 59655 Villeneuve d'Ascq, France

*Author to whom correspondence should be addressed; E-mail: Fhamzaoui@aol.com Tél :+213 45 20 24 77, Fax : +213 45 20 24 77

Abstract: At room temperature, the m-Nitrophenol (m-NPH) appears in two polymorphic structures: orthorhombic and monoclinic forms. In the present work, we shall focus on the monoclinic form of this compound which has a centrosymmetric structure with the space group $P2_1/n$. The molecular dipole moment has been estimated experimentally. High resolution single crystal diffraction experiment was performed at low temperature with MoKα radiation. The crystal structure was refined using the multipolar model of Hansen and Coppens (1978). The molecular electron charge density distribution is described accurately. The study reveals the nature of inter-molecular interactions including charge transfer and hydrogen bonds. In this crystal, hydrogen bonds of moderate strength occur between the hydroxyl group and the O atom in the nitro one.

Keywords: Electron charge density, M-Nitrophenol, XD program, nonlinear optical compound (NLO)

1. Introduction

It is known that m-Nitrophenol crystallizes into two polymorphic forms (monoclinic P21/n and orthorhombic P212121), with four molecules in the unit cell [1-3]. The present work focuses on the structural and electronic charge density study of the molecule of the title compound in the monoclinic phase with the space group P21/n. The structure was first described by Panadares et al. (1975) [4].

To achieve our work we have used the XD package software [5], for a non-spherical atom multipole refinement which has been developed by Hansen and Coppens (1978) [6]. One major component of this package is the program for the least square fitting of multipole model to the experimental data [7-8].

The thermal motion and the structure analysis of the molecule have been performed. The electron density maps have been provided at different sections of the molecule. We also have made available the electron charge distribution around the hydrogen bond and calculated the molecular dipole moment.

Accurate results on the structure and electron charge density distribution of the m-nitrophenol have been exposed in details along this article which highlights the adequacy of the multipolar model and theoretical calculations.

2. Methods

2.1. Spherical X-ray refinement[high order (HO)]

In the atomic center regions where the electron density is less affected by the bonding, the isolated atom model is expected to be a fairly good approximation. The sharp core density has appreciable contribution to reflections at high Bragg angle where the scattering by the more diffuse valence or bond density is negligible. For this latter set of reflections, the X-ray scattering is mainly given by the core electrons contribution. For this reason, a refinement emphasizing the high-order data is expected to yield to atomic parameters less biased by the inadequacy of the spherical-atom model [9]. In order to refine the obtained atomic positions and to determine anisotropic displacement parameters, we have used only high-order reflections with $(\sin\theta/\lambda) \geq 0.75 \text{Å}^{-1}$ and $I/\sigma(I) \geq 3$. This refinement was carried on F^2 with weights calculated as $w = 1/\sigma^2(I)$. The H atoms were found by difference Fourier synthesis and their coordinates were adjusted by extending along the C-H and O-H bond directions to bond lengths of 1.105 Å and 1.029Å respectively.

The X-ray scattering factors for C, N and O atoms comes from the international tables for X–ray crystallography [10] while for H atom the bonded H–atom scattering curve of Stewart, Davidson & Simpson (1965) was used [11].

2.2. Charge Density Multipole Model

The Hansen-Coppens multipole formalism [6], as implemented in the XDLSM least squares program for multipole refinement, was used for both observed and theoretical structure factor fitting. It describes the crystal electron density as a superposition of aspherical pseudo-atoms each modelled on a multipole expansion:

$$\rho_k(\vec{r}) = P_{k,c}\,\rho_{k,c}(\vec{r}) + P_{k,v}\,\kappa^3 \rho_{k,v}(\kappa,\vec{r}) + \sum_{l=0}^{4} \kappa'^3 R_{k,l}(\kappa',\vec{r}) \times \sum_{m=-\ell}^{+\ell} P_{k,lm\pm} Y_{lm\pm}\left(\frac{\vec{r}}{|r|}\right) \qquad (1)$$

Here ρ_c and ρ_v are spherically averaged Hartree-Fock core and valence densities, with ρ_v normalized to one electron. The Slater type radial functions $R_l(r) = N_\ell r^{n_\ell} \exp(-\kappa' \xi_\ell r)$ modulate the spherical harmonic angular functions $Y_{lm\pm}$ and N_l is a normalization factor. The values for parameters $n = n_l$ and ς were chosen according to rules provided by Hansen & Coppens (1978) $n_\ell = 2,2,3,4$ and $\xi\ell = 2.8, 4.0, 5.06\,(\text{Å}^{-1})$ for C, O, N were used respectively for $l = 1,2,3,4$. For the H atoms $n_\ell = 2$ and $\xi\ell = 2\,(\text{Å}^{-1})$ for 1=1, 2.

The sum over *m* in Equation (1) includes $\pm l$, so that for each one, $2l + 1$ functions are included. The adjustable variables are the valence shell contraction-expansion parameters (κ, κ') and the population parameters (P_v, $P_{lm\pm}$). The aspheric charge density was described at the octupole ($l = 3$) level for all non-hydrogen atoms and at the dipole levels ($l = 1$ or 2) for hydrogen atoms not involved and involved in strong H-bonds, respectively. The core and valence scattering factors came from International Tables for X-ray Crystallography (1999) [13]. Charge densities of all hydrogen were considered to have cylindrical symmetry along the corresponding hydrogen-heavy atom bond. A molecular electro-neutrality constraint was applied in all refinements.

To reduce the number of variables, chemical constraints were imposed on the multipole parameters: atoms of similar environment were assumed to have the same deformation electron density. The different local pseudo-atom coordinate systems of the molecule are defined in Figure 1. The multipole and radial (k) parameters of non-H atoms were refined using 1412 reflections with I $\geq$ 3σ(I). The reliability factor obtained is about 0.022.
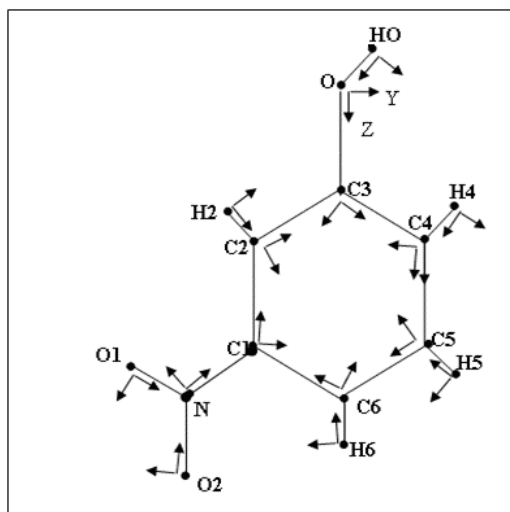

Figure 1. Labeling of the atoms and definition of local orthogonal reference axes for the atom-centered multipolar functions

3. Results and Discussion

3.1. Structural and Thermal vibration analysis

The general features of the structure have been described previously [3]. The main characteristic of this structure is that the four molecules in the unit cell are engaged in four chains formed by infinite chains of hydrogen-bonded coplanar molecules. The H atoms were placed by setting the bond distances C—H and O—H at 1.105 Å and 1.029 Å respectively. Any position error of the hydrogen atom will bring about errors strongly correlated with the dipolar population of hydrogens.

The thermal motion analysis of m-NPH has been performed using the THMA11 program [14]. The rigid-body motion is described by three tensors T, L and S taking into account for translation, libration and the correlation between translation and libration, of the rigid group respectively. These tensors are obtained by a least-squares fit refinement using the observed atomic thermal motion parameters obtained by the refinement. This test indicated that the differences between the mean square displacements of atoms (MSDAs) along interatomic directions have magnitudes $\Delta \leq 10.10^{-4} \text{Å}^2$ for the bonded pairs of the non-H atoms [15]. The MSDAs Δ_{AB} in the AB direction for all pairs of atoms in the molecule have been calculated and reported in Table 1.

Table 1. Matrix for differences in MSDA's (mean square displacements of atoms) [Values listed are 10^4 MSDA's for column atom minus that for row atom, underlined values correspond to chemical bonds].

	O	O2	O1	N	C6	C5	C4	C3	C2
C1	-5	5	2	<u>14</u>	<u>5</u>	17	16	10	<u>-4</u>
C2	-5	27	-9	-1	7	7	8	<u>11</u>	
C3	<u>-10</u>	16	-10	-7	8	5	<u>1</u>		
C4	-19	5	-1	-2	4	<u>4</u>			
C5	-19	-13	0	-7	<u>-4</u>				
C6	-18	-17	5	-3					
N	-4	<u>-15</u>	<u>-7</u>						
O1	2	5							
O2	-40								

In the general treatment of the molecular thermal motion in terms of rigid-body TLS, the calculated anisotropic thermal parameters are given in the Trueblood notation [14] as such:

$$U_{ij} = T_{ij} + G_{ijkl} L_{kl} + H_{ijkl} S_{kl} + D^2 \Omega^2 n_i n_j \tag{3}$$

Where G and H are geometrical parameters and S is an asymmetric tensor needed to account for the average quadratic correlation of T and L. The last term corresponds to any additional intra-libration (Ω) around a chosen axis. The rigid-body fit suggests an independent liberation axis around the C1—N bond. The thermal motion of the H atoms is considered to consist of two contributions. The first is due to rigid molecular motion and the second is from the C—H vibrations [16-18].

The ellipsoids of the different atoms representing their thermal motion described above are shown with an ORTEPIII diagram [19] in Figure 2.
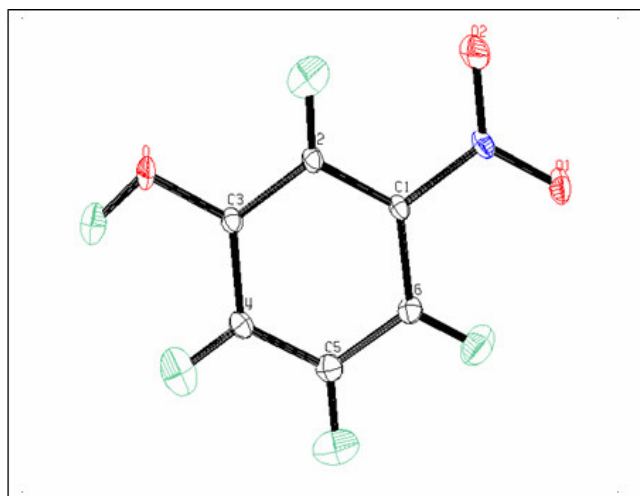

Figure 2. *ORTEPIII* (Johnson, 1996) diagram of the m.Nitrophenol molecule

3.2. Electron-density maps

The aspherical atom model used in multipole refinement gives structure factor phases closer to the true phases for crystals than the spherical or independent atom model does. This enables the mapping of the electron density by Fourier synthesis in various ways using the program XDGRAPH implemented in the XD program package [5].

The experimental density deformation map is shown in Figure 3, from which we can notice the absence of the density on the atomic sites and the appearance of all the bond density peaks and also the localization of the oxygen lone pairs of the nitro group. This map confirms the high quality of the data sets and the efficiency of the formalism used for the data processing as proposed by Blessing [20]. This visualization is obtained using the calculated multipole phases with the observed structure factors F_{obs} *(h)*:

$$\delta\rho^{\,exp}(r) = \frac{1}{V}\sum_{h}\left[\left|F_{Obs}(h)\right|.e^{i\phi_{mul}} - \left|F_{sph}(h)\right|.e^{i\phi_{sph}}\right]e^{-2\pi ih.r} \tag{4}$$

Fsph (**h**) is computed with atomic positions and thermal parameters obtained from the multipole refinement. The electron density deformation obtained from the last refinement is the dynamic model map. This map is obtained from the calculated multipole structure factors, *i.e.* the Fourier coefficients are the difference of two values of F_c:

$$\delta\rho^{\,dyn}(r) = \frac{1}{V}\sum_{h}\left[\left|F_{mul}(h)\right|.e^{i\phi_{mul}} - \left|F_{sph}(h)\right|.e^{i\phi_{sph}}\right]e^{-2\pi ih.r} \tag{5}$$

Temperature factors are included in F_{mul} and F_{sph}. This density distribution is free of experimental noise. Figure 4 shows this electron density deformation, where one can easily observe the obvious

increase of the density peaks and the good localization of the oxygen atoms lone pairs O1 and O2. The presented maps are given in the benzene ring section and the contour map is 0.05 eÅ^{-3}.

A residual density map in the molecular plane obtained in the final cycle of refinement (see Figure 5) shows the adequacy of the multipolar model to describe the electron experimental density of the molecule. The absence of the quasi-totality of the density peak again confirms the high quality of the recorded data and the precision of the used equipment. On the other hand, the multipole expansion model appears to be very efficient for describing the electron density distribution in structure [21-22].
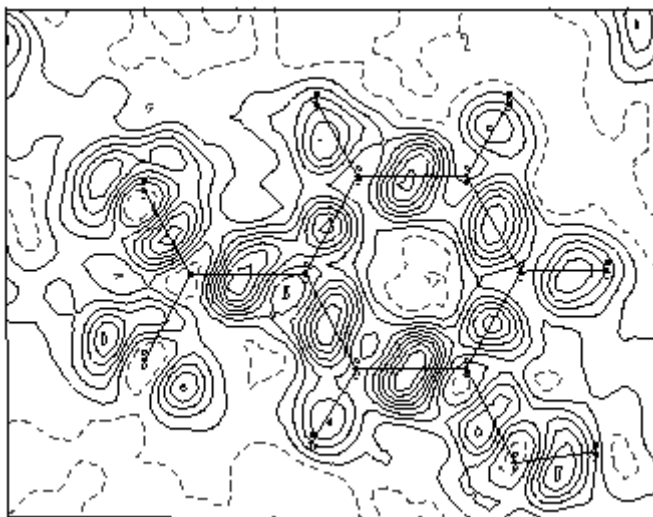

Figure 3. Experimental density map from high-order refinement: $\rho_{\text{exp}} = \rho_o - \rho_{sph}$. ρ_o is the observed electron density and ρ_{sph} is the calculated electron density using the atomic parameters obtained from the high-order refinement. Contour map is 0.05 eÅ^{-3}

Figure 4. Dynamic density map: $\rho_{dyn} = \rho_{mult} - \rho_{sph}$, ρ_{mult} is the calculated electron density using the multipolar model and ρ_{sph} is the calculated electron density using the atomic parameters obtained from the high-order refinement. Contour map is 0.05 eÅ^{-3}
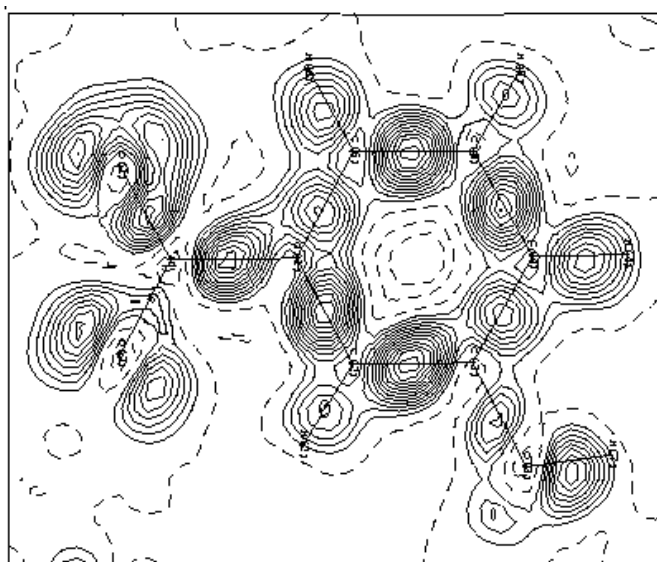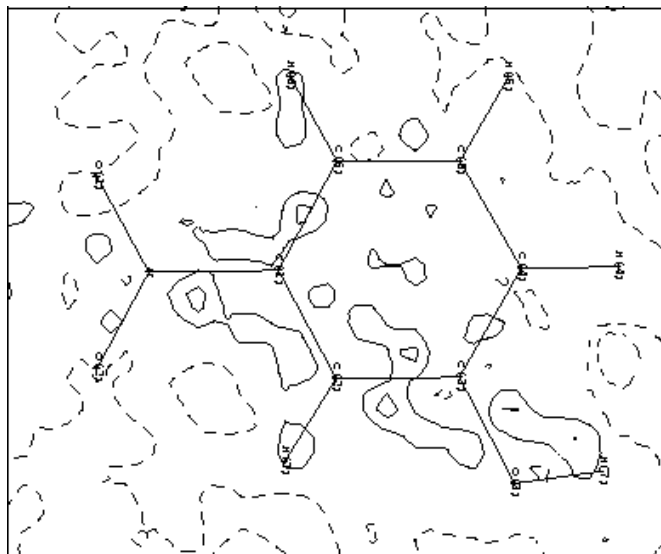
Figure 5. Residual density map: $\rho_{res} = \rho_o - \rho_{mult}$. Contour map is 0.05 eÅ^{-3}

3.3. Molecular dipole moment

The molecular dipole moment was calculated from the multipolar population parameters (Table 2), following the procedure described by Hansen and Coppens (1978) [6]. Values of the multipole parameters are summarized in Table 3. The value of the dipolar moment reaches 5.81 Debye, see Table 4. Its orientation in the molecule is shown in Figure 6. The method is in accordance with the evaluation of the positive sign of the net charges on the H atoms and the negative sign of the net charges on the O atoms.
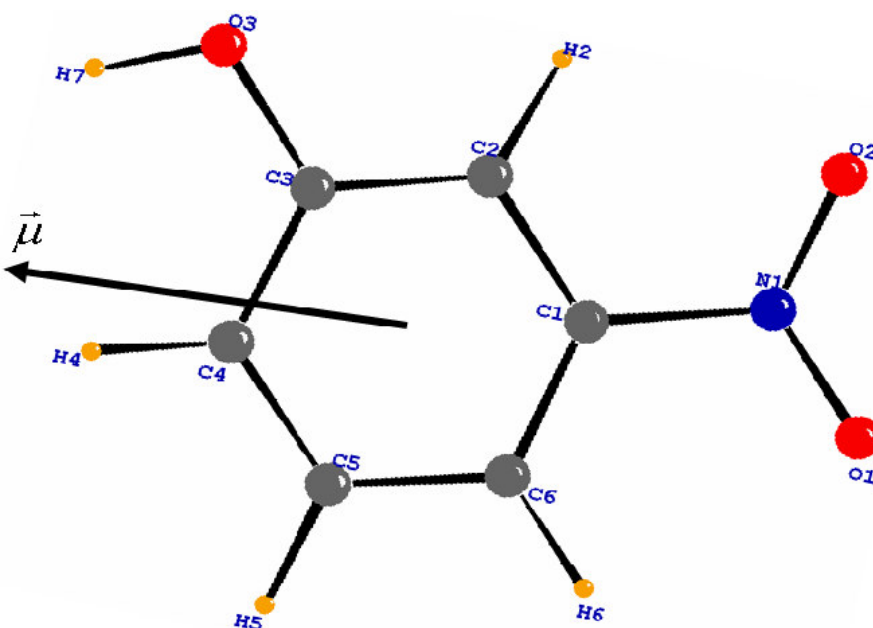

Figure 6. Molecular dipole moment calculated by multipolar model. The origin is at the center of mass of the molecule

Table 2. Net atomic charge in m-Nitrophenol

ATOM	P_v	q
C1	4.153	-0.153
C2	4.270	-0.270
C3	3.971	0.028
C4	4.395	-0.395
C5	4.462	-0.462
C6	4.268	-0.268
N	4.353	0.646
O1	6.233	-0.233
O2	6.218	-0.218
O	6.290	-0.290
H2	0.681	0.318
H4	0.783	0.216
H5	0.749	0.250
H6	0.711	0.288
HO	0.671	0.328

Table 3. The multipolar coefficients as described in the model of Hansen & Coppens. Pv correspond to l=0. d_2 and d_3 correspond to l =1(d1=0) and q_1, q_3 and q_4 are the quadrupolar coefficients corresponding to l=2 ($q_2=q_5=0$). o_1, o_3, o_4 and o_7 are the octapolar coefficients corresponding to l=3 in the multipolar development ($o_2=o_5=o_6=0$). Some coefficients are set equal to zero because of atomic sites symmetries.

Atoms	P_{ml}	d_2	d_3	q_1	q_3	q_4	o_1	o_3	o_4	o_7
C1	4.1536	-0.003	0.082	0.185	-0.001	-0.056	0.212	-0.082	0.175	-0.135
C2	4.2703	0.131	0.354	0.032	-0.027	-0.154	0.265	-0.124	0.192	-0.054
C3	3.9710	0.018	0.197	0.224	0.044	-0.119	0.181	-0.019	0.153	-0.091
C4	4.3953	-0.105	0.114	0.287	0.118	-0.126	0.130	0.040	0.112	0.004
C5	4.4621	-0.037	0.062	0.141	0.025	-0.246	0.165	0.096	0.140	-0.009
C6	4.2681	-0.033	0.008	-0.039	-0.279	0.162	0.224	0.059	0.186	-0.031
N	4.3534	-0.015	0.012	0.050	-0.081	-0.176	0.177	-0.006	0.134	0.033
O1	6.2335	-0.128	-0.055	-0.001	0.003	-0.207	0.056	0.048	0.046	-0.103
O2	6.2179	0.078	-0.073	-0.092	0.111	-0.251	0.068	0.021	0.040	0.098
O	6.2901	-0.036	-0.033	0.068	0.004	-0.052	0.092	-0.018	0.100	0.011
H2	0.6813		0.227							
H4	0.7835		0.281							
H5	0.7492		0.234							
H6	0.7115		0.196							
HO	0.6711		0.126							

Table 4. Magnitude of the molecular dipole moment

μ_x	μ_y	μ_z	μ (Debye)
-0.032	-0.032	-0.636	5.81 (20)

3.4. Hydrogen bonds

The crystal structure of the mNPH rests on chains of molecule joined by hydrogen bonds, the almost linear hydrogen bonding links by translation of equivalent molecules along the c crystallographic axis through the OH and NO_2 groups (see Figure 7). Hydrogen atoms are positioned to give 1.105 and 1.029 Å C—H and O—H bond**s** lengths, respectively. The O—H----O distance is a little shorter in the orthorhombic crystal (2.88Å), than in the monoclinic structure (2.94Å). On the other hand the O—H----O angles differ slightly: 168° and 178° in both polymorphic structures respectively. There are nine intermolecular interactions which are possible in the hydrogen bond network as shown in table 5.
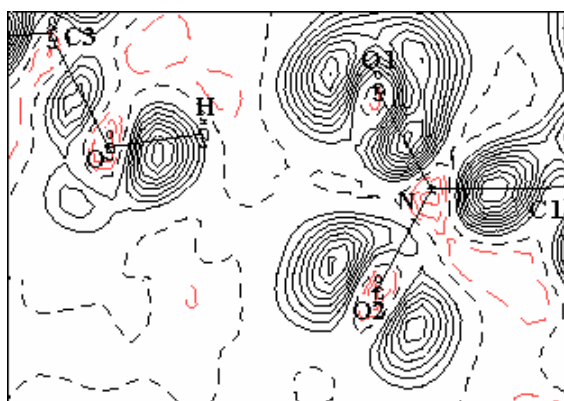
Figure 7. Deformation density map in the plan of the hydrogen bond; Contour map is 0.05 eÅ^{-3}

Table 5. Various possible hydrogen bonds

D —H ...A	*D —H...A (°)*	*D —H (Å)*	*D...A (Å)*	*H....A (Å)*
C2—H2…..O2 (a)	95.26 (8)	1.105 (2)	2.717 (3)	2.382 (3)
C6—H6..…O1 (a)	91.79 (9)	1.093 (2)	2.727 (3)	2.464 (2)
C4—H4…..O1 (b)	129.70 (9)	1.094 (2)	3.386 (4)	2.581 (3)
O —HO…..N (b)	155.47 (8)	1.029 (1)	3.495 (4)	2.532 (3)
O —HO…..O1 (b)	178.03 (8)	1.029 (1)	2.908 (3)	1.880 (2)
O —HO......O2 (b)	127.49 (8)	1.029 (1)	3.315 (4)	2.586 (3)
C5—H5…..O1 (c)	124.62 (9)	1.109 (2)	3.693 (5)	2.949 (4)
C5—H5…..O2 (d)	140.67 (9)	1.109 (9)	3.338 (3)	2.405 (2)
C5—H5…..O (e)	131.87 (9)	1.109 (2)	3.471 (3)	2.631 (2)

Symmetry operations :

(*a*) *x, y, z*   (*b*) *x, +y, +z*-1   (*c*) -*x*+2, -*y*+1, -*z*+1

(*d*) *x*+1/2, -*y*+1/2, +*z*-1/2   (*e*) *x*+1/2, -*y*+1/2, +*z*+1/2

4. Experimental Section

The crystallographic data were obtained at 122K on a CAD4 diffractometer using the graphite–monochromated MoKα radiation. The crystal of high quality was cooled by using a modified Enraf Nonius nitrogen gas-flow system. The cell parameters were determined from refinement by using centered angular positions of 25 reflections with $11 \leq \theta \leq 25°$. The profiles of the different reflections were measured using θ -2θ step scan method. A total of 3148 intensities were recorded up to two theta of 116°. Only selected reflections with significant intensity were collected for reflections in the [0°-58.85°] theta range. A number of 1736 independent reflections of which 1412 were used in the refinement procedures.

The H atoms were located by difference Fourier synthesis as described in section 2.1. The data reduction and error analysis were carried out by using the programs of Blessing (1989) [21]. The experimental details and crystal data are displayed in Table 6. The crystal structure has been deposited at the Cambridge Crystallographic Data Centre with the deposition number CCDC 275138. These data can be obtained free of charge from The Cambridge Crystallographic Data Centre via www.ccdc.cam.ac.uk/data_request/cif.

5. Conclusion

This study has obtained good accurate results on the structure and electron charge density which gives high quality descriptive model for the electron charge density distribution from X-ray diffraction experiment. It also revealed that electron density can yield to electronic proprieties such as dipole moment.

According to the orientation of the molecular dipole moment, the region of the nitro and hydroxyl groups is electronegative, whereas the region of the C-H groups is electropositive.

The coplanarity of the hydrogen bonded molecules together with the donor-acceptor interactions across the molecules probably enhance the nonlinear response of the orthorhombic mNPH, as it was discussed recently in case of the other nitrobenzene derivative [23]. In the monoclinic mNPH, the centrosymmetry of the crystal cancels the nonlinear response.

Finally, our results could be analyzed in more detail, if they were completed by quantum chemistry calculations. Especially, for the explanations about the existence of the polymorphism in m–Nitrophenol compounds.

Table 6. Experimental details

Crystal data	
Chemical formula	$C_6H_5NO_3$
Chemical formula weight	139.11
Cell setting	Monoclinic
Space group	$P2_1/n$
a (Å)	11.026(4)
b (Å)	6.736(1)
c (Å)	8.119(21)
β (°)	97.73 (2)
V (Å^3)	597.50
Z	4
D_x(mg m^{-3})	1.54
Radiation type	Mo $K\alpha$
Wavelength (Å)	0.71073
No. of reflections for cell parameters	25
θ range (°)	11 – 25
μ (mm^{-1})	0.127
Temperature (K)	122 (1)
Crystal form	Prism
Crystal size	$0.10 \times 0.27 \times 0.32$
Crystal color	Colorless
Data collection	
Diffractometer	Nonius CAD-4
Data collection method	$\theta - 2\theta$
$2\theta_{max}$	117.71
No. of measured reflections	3148
No. of independent reflections	1736
No. of observed reflections	1412
Criterion for observed reflections	$I \geq 3\sigma(I)$
R_{int}	0.021
Range of h, k, l	$-25 \rightarrow h \rightarrow 23$
	$0 \rightarrow k \rightarrow 15$
	$0 \rightarrow l \rightarrow 18$
No. of standard reflections	3
Frequency of standard reflections	Every 120 min

Refinement				
	N	R	wR	S
Spherical refinement	92	0.038	0.040	1.02
Multipole refinement	221	0.022	0.035	1.12

N is the number of refined parameters and M is the number of observations. $R = \sum |F_o| - |F_c| / \sum |F_o|$; $wR = \left[\sum w \left(|F_o| - |F_c| \right)^2 / \sum w |F_o|^2 \right]^{1/2}$; $S = \left[\sum w \left(|F_o| - |F_c| \right)^2 / (M - N) \right]^{1/2}$

Source of atomic scattering factors	*International Tables for X-ray Crystallography* (1999, Vol. C)

References

1. Hamzaoui, F.; Baert, F.; Wojcik, G. Electron-density study of *m*-nitrophenol in the orthorhombic structure. *Acta Cryst. B* **1996**, *52*, 159-164.
2. Wojcik, G.; Marqueton, Y. The phase transition of m-nitrophenol. *Mol. Cryst. Liq. Cryst.* **1989**, *168*, 247-254.
3. Wojcik, G.; Toupet, L. The inter-and intramolecular charge transfer along the polymeric chain of hydrogen-bonded molecules in two crystal forms of m-nitrophenol. *Mol. Cryst. Liq. Cryst.* **1993**, *229*, 153-159.
4. Panadares, F.; Ungaretti, L.; Coda, A. The crystal structure of a monoclinic phase of *m*-nitrophenol. *Acta Cryst. B* **1975**, *31*, 2671-2675.
5. Koritsanszky, T.; Howard, S.; Richter, T.; Su, Z.; Mallinson, P.R.; Hansen, N.K. XD a Computer Program Package for Multipole Refinement and Analysis of Electron Densities from Diffraction Data. Free University of Berlin, Berlin, Germany, **2003.**
6. Hansen, N.K.; Coppens, P. Testing aspherical atom refinements on small-molecule data sets. *Acta Cryst. A* **1978**, *34*, 909-921.
7. Volkov, A.; Abramov, Y.; Coppens, P.; Gatti, C. On the origin of topological differences between experimental and theoretical crystal charge densities. *Acta Cryst. A* **2000**, *56*, 332-339.
8. Volkov, A.; Gatti, C.; Abramov, Y.; Coppens, P. Evaluation of net atomic charges and atomic and molecular electrostatic moments through topological analysis of the experimental charge density. *Acta Cryst. A* **2000**, *56*, 252-258.
9. Jeffrey, G.A.; Cruickshank, D.W.J. Molecular structure determination by *X*-ray crystal analysis: modern methods and their accuracy**.** *Quart. Rev. Chem.Soc*. **1953**, *7*, 335-376.
10. *International Tables for X-ray* Crystallography, Kynoch Press, Birmingham, **1962**, Vol.III.
11. Stewart, R.F.; Davidson, E.R.; Simpson, W.T. coherent X-Ray Scattering for the Hydrogen Atom in the Hydrogen Molecule. *J. Chem, Phys.* **1965**, *42*, 3175-3187.
12. Coppens, P. X-ray Charge Densities and Chemical Bonding. New York: Oxford, **1997**.
13. *International Tables for X*-ray *Crystallography*. Kluwer Academic Publishers, **1999**, *Vol C*.
14. Trueblood, K.N. *Program THMAI1*, Department of chemistry and biochemistry, University of California, Los Angeles, **1990**.
15. Hirshfeld, F.L. Can X-ray data distinguish bonding effects from vibrational smearing?. *Acta Cryst. A* **1976**, *32*, 239-244.
16. Hirshfeld, F.L. Difference densities by least-squares refinement: fumaramic acid. *Acta Cryst B* **1971**, *27*, 769.
17. Hirshfeld, F.L. Bonded-atom fragments for describing molecular charge densities. Theor.Chim Acta **1977**, *44*, 129.
18. Hirshfeld, F.L.; Hope, H. An x-ray determination of the charge deformation density in 2-cyanoguanidine. *Acta Cryst. B* **1980**, *36*, 406.
19. Johnoson, C.K. ORTEP program. Report ORNL-3794, Oak Ridge National Laboratory, Tennessee, **1965**.
20. Blessing, R.H. DREAD - data reduction and error analysis for single-crystal diffractometer data. *J. Appl. Cryst*. **1989**, *22*, 396-397.

21. Souhassou, M.; Blessing,R.H. Topological analysis of experimental electron densities. *J. Appl. Cryst* **1999**, *32*, 210-217.

22. Souhassou, M.; Lecomte, C.; Blessing, R.H; Aubry, A.; Rohmer, M.M.; Wiest, R.; Benard, M.; Marraud, M. Electron distributions in peptides and related molecules.1. An experimental and theoretical study of N-acetyl-L-tryptophan methylamide. *Acta Cryst. B* **1991**, *47*, 253-266.

23. Wojcik, G.; Holband, J.; Szymczak, J.J.; Roszak, S.; Leszczynski, J. Interactions in Polymorphic Crystals of m-Nitrophenol as Studied by Variable-Temperature X-ray Diffraction and Quantum Chemical Calculations. *Crystal Growth & Design* **2006**, *6*, 274-282.